

CERN/PS 88-77 (OP/PA)
December 1988

SIMULATION OF THE PS SLOW EXTRACTION 62 WITH THE MAD PROGRAM

Francesca Galluccio*
Thys Risselada, Charles Steinbach
and M. (Sanki) Tanaka**

Geneva, Switzerland

* Visitor from INFN, Sezione di Napoli

** Visitor from BNL AGS

ABSTRACT

A new proposal for the PS slow extraction has been examined by simulation using the computer program MAD. The present report describes a method developed for the modeling of the PS main magnet field. The agreement between the simulation and the tune measurements and beam observations using the present scheme is shown to be satisfactory. The application and the results of this method to predict the properties of the proposed new scheme are presented and discussed.

1. INTRODUCTION

A new layout for the slow extraction to the PS East Hall has been proposed by C. Steinbach in 1986 [1], which offers several advantages over the present scheme:

- there are only two septa inside the vacuum instead of four
- these septa are located at the inner side of the vacuum chamber (towards the center of the ring), which exposes them less to the synchrotron radiation emitted by the electron and positron beams
- less straight section space is required

The proposal was based on a simulation performed with a simplified model including only the quadrupolar and sextupolar components of the main PS magnet. Therefore a study was undertaken in order to test the feasibility of the new scheme with more accuracy. The existing extraction, designed in 1971 [2, 3], was first simulated and compared to observations in order to assess the validity of the method. The new scheme was then studied starting from the predictions of reference [1]. This note presents the results and describes the method used to calculate the optics of the extraction. The results of highest interest are the clearance at the first magnetic septum, the horizontal beam size at the first quadrupole of the ejected beam line and the vertical emittance blow-up during the traversal of the non linear fringe field. The main machine parameters for each case are listed below.

In combined function machines the fields in the main magnet units at large radial positions (in the present case 100 mm and more) away from the central orbit are obviously very non-linear. The MAD program [4] was used to track particles first on the resonance up to the electrostatic septum, and from there through the stray field of the main bending magnets into the ejection line. MAD allows multipoles up to 20-pole (K9), which is just about sufficient in the present problem. The field description was based on recent measurements of the PS main bending magnet with the real poleface winding currents corresponding to the present and the future slow ejection working point.

1.1 Parameters of the present scheme (see layout on fig. 1a)

Main Magnets : 4732 A 1.1514 T

PFW's

IPFWF	: 78 A	For $Q_h = 6.26$, $Q_v = 6.24$
IPFWD	: 75 A	and $Q_h'/Q_h = -1.7$
IPFW8	: 0 A	

Bumps

BSW83	: 335 A	BNO80+BNO82/2+BNO88+BNO90/2
BSW62	: 426 A	BLG59 - BLG75

SE Magnets

QSE23+53	: -385 A	2 Quads of type 409
XSE53	: -653 A	1 Sext of type 608

Septa

SES83	: 150 kV	$x(\text{anode}) = 72.0$ mm, $x(\text{cathode}) = 89.0$ mm
SMH85	: 2100 A	
SMH61+62	: 8675 A	

1.2 Parameters of the proposed scheme (see layout on Fig. 1b)

Main Magnets : 4732 A 1.1514 T

PFW's

IPFWF	: 77 A	For $Q_h = 6.21$, $Q_v = 6.33$
IPFWD	: 88 A	and $Q_h'/Q_h = -1.1$
IPFW8	: 0 A	

Bumps

BSW23	: 600 A	-DNH206(19)-DNH206(27)
BSW57+61	: 500 A	-DNH206(53)+DNH206(59)-DNH206(61)+DNH206(67)

SE Magnets

QSE29+87	: 610 A	Q409(29)+Q409(87)
XSE7+19	: 260 A	1 Sext ISR 41.0 T/m in SS07
		2 Sexts 608 14.6 T/m in SS19

Septa

SES23	: 150 kV	$x(\text{anode}) = 72.0$ mm, $x(\text{cathode}) = 89.0$ mm
SMH57	:	KICK = 3.9 mrad
SMH61	:	KICK = 1.2 mrad

2. MODELLING OF THE PS WITH THE MAD PROGRAM

A first simulation of the PS slow ejection was made using field data obtained with the Poisson program [5]. However this calculation could not reproduce the measured working point with sufficient precision. It was therefore decided to make magnetic field measurements on a PS spare main magnet unit, using the poleface winding current settings of the present and future slow ejection schemes [6].

Another problem was to convert these measurements into multipole strengths as required by MAD. Finally a way was found [7] to describe the working point with sufficient precision by fitting multipole coefficients to the measured field values over a limited range of radial positions. The ejection tracking had to be carried out in 3 steps, each step using a separate field description, obtained by least square fit multipole analysis over a well defined range:

- simulation of the circulating beam up to the first electrostatic septum was done using multipole analysis of the range -50 to +50 mm, which gives a good agreement with the measured tunes and chromaticities. Only multipole coefficients K0 to K5 (dipole to 12-pole) are non-zero.
- simulation of the beam in the last turn from the first septum to the last septum was made using an analysis of the range -100 to +100 mm, using all multipole coefficients K0 to K9 (dipole to 20-pole).
- for the traversal of the stray field downstream of the last septum (positions varying between +100 and +250 mm from the central orbit) a local analysis was made, centred around the ejected beam trajectory, containing a dipole, a quadrupole and a sextupole component.

2.1 MAD input data sets

The following MAD data sets (all files have type "MADSAVE" and have been filed in user "PSRING" in the IBM (CERNVM)) were required to describe the existing slow ejection scheme at the PS.

PSRING:

The complete PS ring. It defines the layout of around 900 machine elements of the PS. The main magnets contain only multipoles up to sextupole (K0, K1 and K2 in MAD).

PSEJECT:

It defines extraction lines, including SE62. It introduces higher multipoles K3, K4, .. ,K9 (K9 is the highest allowed in MAD) as thin lenses at both ends of each main magnet half unit. This adds another 400 elements to the machine.

HEB5:

It defines the geometry of the main combined function magnets F and D and contains a table of multipole coefficients up to order 5 (K0, K1, .., K5) valid for the High Energy working point HEB which is in operation on the B cycles used for slow ejection at 24 GeV/c. The coefficients were obtained by fitting the measured fields in the range from -50 mm to + 50 mm with respect to the reference orbit. K6 to K9 are set to zero.

HEB9:

The same as HEB5, except that it contains non-zero coefficients up to K9, obtained by fitting the field data between -100 mm and + 100 mm.

STRAY62:

It defines the stray field at magnet unit BHZ62 D and F on the ejection trajectory just downstream of the septum 62, i.e. at radial positions between +100 and +160 mm in the D half-unit, and between +160 and +230 mm in the F half-unit. In order to make a good quality fit the analysis is centred around the trajectory of the ejected beam, and not around the central orbit. To this end a change of coordinate system is applied in MAD by means of two successive HKICK elements:

```

ROT1 : HKICK, KICK = -0.363
DR   : DRIFT, L   = 0.3
ROT2 : HKICK, KICK = +0.348

```

3. THE PRESENT SCHEME

3.1 Tune measurements at 24 GeV/c

Tune measurements were performed on the bare machine as well as on the machine with the slow ejection SE62 elements excited in order to get information about the third integer slow extraction working point. The machine tune Q_h and Q_v were obtained as a function of the mean beam position ($\langle x \rangle$) using the Q-meter and the closed orbit measurement program. The bare machine was defined as a machine at $p = 24.0$ GeV/c, IPFWF = 78 A and IPFWD = 75 A without turning on any SE62 equipments.

Fig. 2a shows measured Q_h & Q_v values as a function of the mean radial beam position $\langle x \rangle$ for the bare machine and the MAD calculations using a field map, HEB5 (the solid lines). Then the machine was set up for SE62 with parameters:

XSE53 = -653 A, QSE23&53 = -368 A, BSW83 = 335 A and BSW62 = 426 A

Fig. 2b shows measured values of Q_h & Q_v versus $\langle x \rangle$ for the machine during the flat top at 24 GeV/c together with the MAD calculations using HEB5 (solid lines).

3.2 Working point parameters used in MAD

MAD input data set HEB5 contains the geometry of the PS main magnet units at 24 GeV/c. Two 'free' parameters describing the integrated quadrupole and sextupole fields in the junction between F and D half-units, which have not yet been measured, are adjusted to fit the observed bare machine condition as shown in Fig.1a.

Then the bumpers, quadrupoles and sextupoles are turned on and the third integer resonance $3*Q_h = 19$ is excited.

The MAD predictions are in good agreement with the observed SE62 working point as seen in fig. 1b. Note that $\langle x \rangle$ is calculated from the formula:

$$\langle x \rangle = \text{delta}(s)/2.\pi$$

where $\text{delta}(s)$, calculated by MAD, is the length difference between the particle orbit and the reference orbit.

Particle tracking in the horizontal plane has been performed with MAD under the above mentioned conditions for a zero emittance ($E = 0$) and a nominal emittance ($E = 0.8 \pi \text{ mm.mrad}$) beam as the observed beam emittance is $0.5 < E < 1.0 \pi \text{ mm.mrad}$.

3.3 Tracking of the resonance

During the slow extraction process the particles travel many turns between the extreme inside and the extreme outside of the vacuum chamber and their orbits are quite sensitive to non-linear fields. When leaving the machine the beam has to go through the fringe field. Tracking has been done in two steps: first the circulating beam and then the last turn starting at the electrostatic septum.

Up to the first (electrostatic) septum SES83 ($x = 72 \text{ mm}$) tracking uses datafile HEB5 (circulating particles). Fig. 2a shows x' vs x (phase space) at the entrance of SES83 for $dp/p = 0.00408$ ($E = 0$) and for $dp/p = 0.00376$ ($E = 0.8 \pi \text{ mm.mrad}$).

During the extraction process the stability of particles depends both on their momentum and betatron amplitude: for each momentum there is an emittance threshold above which the particles are unstable. The machine field is slowly swept so that each particle ends up sooner or later on the separatrix.

The $\text{delta}p/p$ values corresponding to nominal and zero emittance have been found by trying to go as close as possible to the third integer resonance ($Q_x = 6.33333$) for the zero emittance case, and by trying out different sets of initial values for the case of the nominal emittance.

Tracking runs were made for each case, adjusting the initial conditions in small steps to find two adjacent trajectories corresponding to the largest stable and the smallest unstable emittance.

From the stable particle tracking (fig. 3 a) the emittance was roughly evaluated, taking the coordinates of the stable triangle vertices from the graphic output, and calculating as follows:

$$E = 0.5 (X_1(X_3 - X_2) + X_2(X_1 - X_3) + X_3(X_2 - X_1))$$

The unstable particle tracking was used to compute the spiral pitch: tracking was stopped as soon as the particle had jumped the septum. The positions of the successive turns were interpolated along the extracting separatrix so as to find the value of x' at the position of the septum ($x = x_s = 72$ mm). Tracking was then resumed with starting conditions $x = x_s$ and $x' = x'(x_s)$.

3.4 Tracking of the extracted beam

From the first (electrostatic) septum SES83 to the final ejection septum SMH62 and from SMH62 to SS63 (stray field) the MAD tracking uses HEB9 (last turn before ejection) and STRAY62 (stray field). The particles passing outside the SES83 septum are kicked further outside and receive the following kicks:

```
SES83: HKICK, KICK= 0.00028, L=1.0
SMH85: HKICK, KICK=-0.00125, L=1.0
SMH61: HKICK, KICK= 0.00340, L=1.2
SMH62: HKICK, KICK= 0.00909, L=1.0
```

At + 110 mm the gradient in the F half unit changes sign, and around +150 mm its value is equal to - 3 times the nominal (central orbit) value. Beyond + 200 mm the gradient returns to zero. For this reason it is not possible to find a multipole development covering the entire range - 100 to + 300 mm with sufficient accuracy. Downstream of the last septum the multipole analysis has to be performed over a limited range centered around the ejected beam trajectory, as shown in data set STRAY62 (see chapter 2):

```
half unit 62-D: range + 110 to + 160 mm (offset + 135 mm)
half unit 62-F: range + 160 to + 230 mm (offset + 195 mm)
```

The offset implies a change of reference system, obtained by using two HKICK elements separated by a drift (this introduces a small dispersion error, which may be neglected). The beam positions calculated by MAD are expressed with respect to the new reference system. After the second HKICK the beam passes through the elements of the transfer line with positions close to zero.

3.5 Results

The following figures and table shows numerical results of the MAD tracking with the present scheme:

Fig. 3b x' vs x at the exit of SES83
 Fig. 3c x' vs x at the exit of SMH85
 Fig. 3d x' vs x at the exit of SMH61
 Fig. 3e x' vs x at the exit of SMH62

	E = 0		E = nominal	
Qh	6.33137		6.33541	
Xh	-1.8		-1.8	
dp/p	0.00408		0.00376	
E [pi mm.mrad]	0.007		0.817	
	x [mm]	x' [mrad]	x [mm]	x' [mrad]
SES83	41.107	0.467	32.171	0.308
(fixed	41.749	0.506	40.408	0.732
points)	42.546	0.485	48.193	0.489
at septum	72.000	0.835	72.000	0.758
Starting points	72.050	0.835	72.050	0.758
SES83 entrance	78.450	0.922	80.703	0.865
SES83 (exit)	73.021	1.115	72.995	1.038
	79.508	1.202	81.704	1.145
SMH85 (exit)	71.853	-2.301	70.379	-2.390
	78.027	-2.414	78.589	-2.550
SMH61 (exit)	95.465	5.049	97.944	5.304
	97.900	4.997	101.50	5.365
SMH62 (exit)	103.48	13.70	105.14	13.65
	107.21	14.06	110.75	14.22
BHZ62D (exit)	xmin = 148.		xmax. = 164.	
BHZ62F (exit)	= 208.		= 221.	
spiral pitch at				
SES83 entrance				
dx [mm]	6.4		8.7	
dx' [mrad]	0.088		0.107	

3.6 Comparison with measurements

From the above results, one can deduce the calculated beam sizes and separation between extracted and circulating beam (clearance at the septum locations):

	Beam width [mm]	Clearance [mm]
SES83	8.7	
SMH85	8.2	2.2
SMH61	6.0	28.0
SMH62	7.0	45.9
QFO01(Ent.)	17.	
TV02	41. with QFO01 = 0 A	
	22.	= 300
	4.	= 610

Some of the beam sizes can be directly observed on luminescent screens. Fig.4 shows the real beam spots on TV02 for various current values of QFO01.

Though it is difficult to make any quantitative comparison it appears that these simulation results with MAD reasonably agree with the experimental observations for the present scheme. It seems therefore natural to extend this simulation study with MAD to the new proposed scheme.

4. THE PROPOSED NEW SCHEME

4.1 Tune measurements at 24 GeV/c

Tune measurements were similarly performed on the bare machine of the proposed new scheme in order to establish a reference situation for comparison with the MAD simulation. The machine tunes Q_h and Q_v were measured as a function of the mean beam position ($\langle x \rangle$) using the Q-meter and the orbit measurement program. The bare machine was defined as a machine at $p = 24.0$ GeV/c, IPFWF = 77 A and IPFWD = 88 A without turning on any equipment installed for the new ejection scheme.

Fig. 5a shows measured Q_h & Q_v values as a function of the mean radial beam position $\langle x \rangle$ for the bare machine, as well as the MAD predictions for this case, using the data set HEB5NEW described in 4.2 (the solid lines). Since the machine could not yet be set up for the new ejection scheme, only the MAD predictions are shown in Fig. 5b.

4.2 Working point parameters used in MAD

In addition to PSRING, PSEJECT, the following datasets are required to describe the machine with the new ejection scheme:

PS62NEW:

It defines the elements used in the new ejection scheme and the modified PS ring layout.

HEB5NEW:

It defines the geometry of the main magnet and has a table of multipole coefficients up to 5 poles (K_0, K_1, \dots, K_5) for the main magnets obtained by fitting the field data between -50 mm and + 50 mm. The poleface winding settings for the new scheme are slightly different from the ones used with the present scheme. Both magnetic field measurements and tune measurements have been made for this new working point.

HEB9NEW:

The same as HEB5NEW except that it has non-zero coefficients up to K_9 using the field data between - 100 and + 100 mm.

STRAY62NEW:

The stray field in magnet unit 62 on the ejection trajectory of the new scheme.

4.3 Tracking with MAD

Junction parameters were again used to fit the measured working point. The tracking was made with the following conditions:

- a) Up to SES23 ($x = -72$ mm) using HEB5NEW

Fig. 6a x' vs x at the entrance of SES23

- b) From SES23 to SMH61 using HEB9NEW and from SMH61 to SS63 using STRAY62NEW:

SES23: HKICK, KICK=-0.00028, L=1.0

SMH57: HKICK, KICK= 0.00390, L=1.0

SMH61: HKICK, KICK= 0.00120, L=1.2

4.4 Results

A first run was performed starting from the data of reference [1]. The corresponding sextupole current was 210 A. This gave a spiral pitch (beam size) of 7.5 mm and a clearance at SMH 57 of 4 mm, both too small. It was then decided to increase the sextupole current to 260 A.

The results of tracking with the proposed new scheme are summarized in the following figures and tables, valid with XSE = 260 A:

Fig. 6b x' vs x at the exit of SES23

Fig. 6c x' vs x at the exit of SMH57

Fig. 6d x' vs x at the exit of SMH61

	E = 0		E = nominal	
Qh	6.33290		6.32870	
dp/p	0.00234		0.00310	
Xh	-0.77		-0.77	
E [pi mm.mrad]	0.001		0.627	
	x[mm]	x'[mrad]	x[mm]	x'[mrad]
SES23	-46.450	-0.132	-49.171	-0.390
(fixed	-46.466	-0.119	-49.487	-0.031
points)	-46.079	-0.119	-38.484	-0.054
at septum	-72.000	-1.059	-72.000	-1.226
starting points	-72.050	-1.059	-72.050	-1.226
SES23 entrance	-83.158	-1.513	-82.613	-1.654
SES23 (exit)	-73.247	-1.339	-73.412	-1.506
	-84.807	-1.793	-84.401	-1.934
SMH57 (exit)	-68.633	3.776	-69.270	3.686
	-83.710	3.679	-83.449	3.580
SMH61 (exit)	120.162	7.060	120.427	7.200
	117.399	7.587	117.459	7.680
spiral pitch at				
SES23 entrance				
dx [mm]	10.61		11.16	
dx' [mm.mrad]	0.428		0.453	
	BetaV	AlphaV	BetaV	AlphaV
Vertical Twiss	107.268	-13.588	114.532	-14.594
parameters TV2	127.424	-16.470	124.048	-16.131
	SES23	SMH57	SMH61	QFO01
Beam width, dx[mm] :	11.6	15.7	3.0	11.0
Clearance, dg[mm] :	-	6.1	52.1	

5. CONCLUSIONS

A simulation study was performed of the present slow extraction at the PS, as well as a study of the proposed new scheme, by means of particle tracking with the MAD program.

A method has been found to simulate particles under the most extreme conditions, which not only allows predicting properties of the proposed new slow extraction scheme, but also provides a general tool valuable for studies of all kinds of slow and fast extraction.

For the study a description of the PS main magnet field was used containing multipoles up to 20-pole (K9). The multipole strengths were obtained by fitting recent field measurement data on a PS spare magnet unit. Three different multipole tables had to be used: one for the case of the circulating beam, one for the last turn tracking and one for the traversal of the PS main magnet stray field.

There is a good agreement between the MAD results and the experimental observations of the present extraction, which means that the model used is realistic and one may have confidence in the predictions for the beam widths and positions of the new scheme.

The clearance at the first magnetic septum, a key parameter for a good efficiency, is calculated to be 6.1 mm, smaller than expected [1]. However, the results show that with a more careful adjustment of the current in the sextupoles, one can increase it to 6.7 mm. This can still be further improved by lowering the Q_h value with the help of the pole face winding currents, and increasing QSE, the current in the quadrupoles (This increases the horizontal beta function at both first septa).

The horizontal beam width at the first quadrupole downstream of the ejection septum (QF001) is an important parameter, as this quadrupole will be rebuilt for the new scheme. It is found to be 30 % smaller in the new scheme: 11 mm total width instead of 17 mm. The comparison with the results of reference [1] shows the importance of the higher order multipoles in the tracking at large amplitudes.

As for the vertical blow-up, it is deduced from the four different vertical Twiss parameters, through the calculation of the circumscribing ellipse. This shows a 23% blow-up, much better than expected, the difference being explained by the fact that the horizontal size is small in the perturbed region of magnets 61 and 62.

6. ACKNOWLEDGEMENTS

We would like to thank R. Cappelletti for confirming our Q measurement results by the FFT method and E. Schulte for his dedicated work on the Q-meter and the pick-up electrodes. We also thank J.P. Riinaud and D. Simon for fruitful discussions and suggestions during this work. Two of the authors (F.G. and M.T.) would like to express their appreciation of the warm hospitality they have received during their stay at the CERN PS division.

7. REFERENCES

1. Ch. Steinbach, "Proposal for a new PS slow extraction", PS/OP/NOTE 86-24.
2. W. Kubischta, Lay-out of elements for SE 16, CERN/MPS/DL 71-5
3. D. Dumollard et D.J. Simon, "Trajectoires et optique du faisceau SE62 dans le Champ de fuite du PS", PS/MU/EP/Note 78-3.
4. F.C. Iselin and J. Niederer, "The MAD Program", CERN/LEP-TH/88-38
5. Y. Ma, private communication
6. G. Suberlucq, to be published
7. T. Risselada, "The optics of the fast ejections of the CERN PS", to be published.

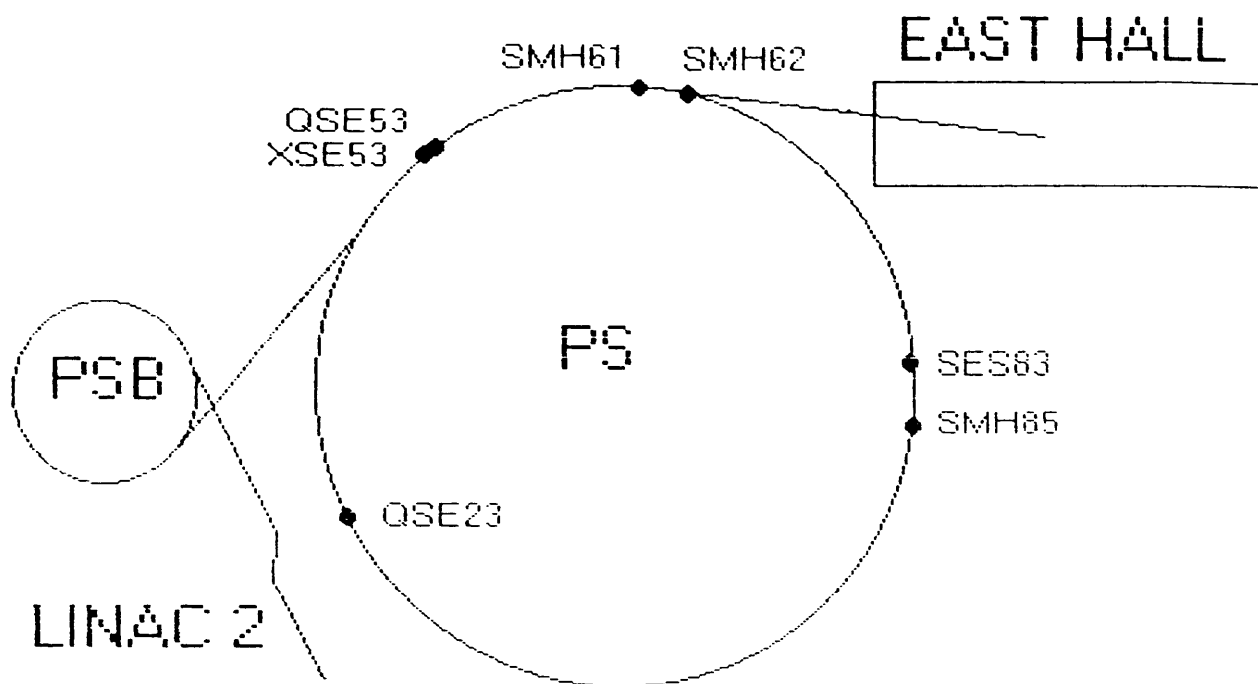


Fig. 1 a - Slow Extraction 62: Present Scheme

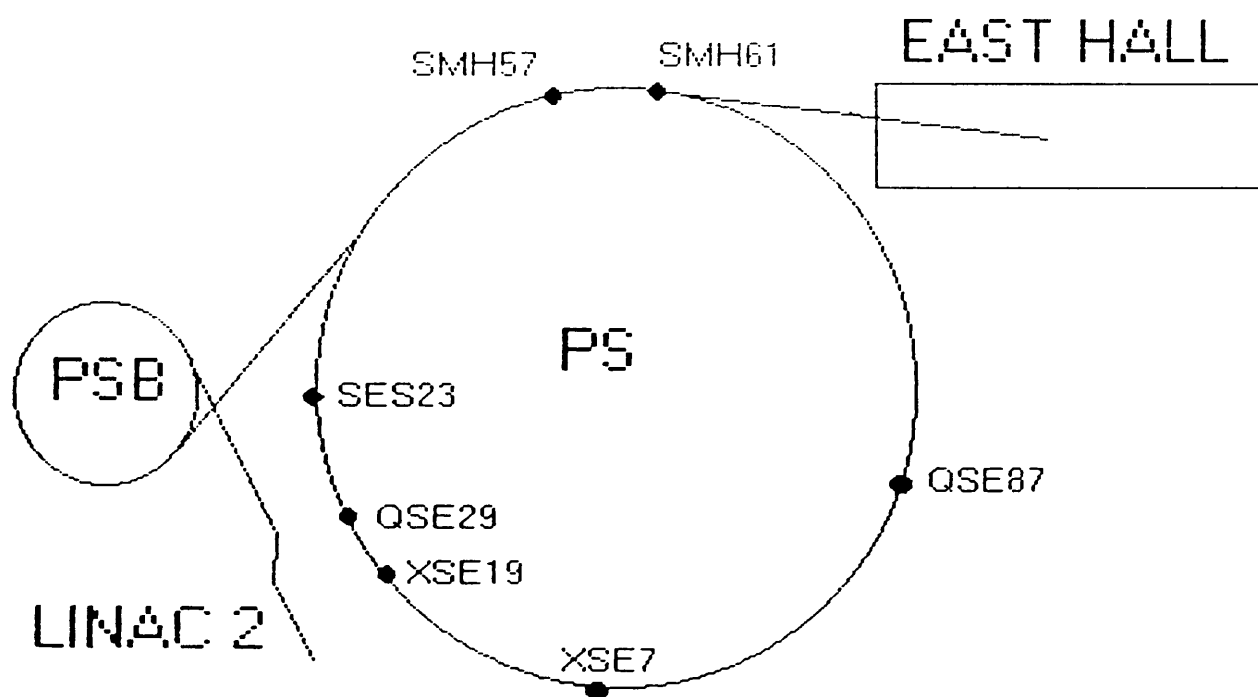


Fig. 1 b - Slow Extraction 62: Proposed scheme

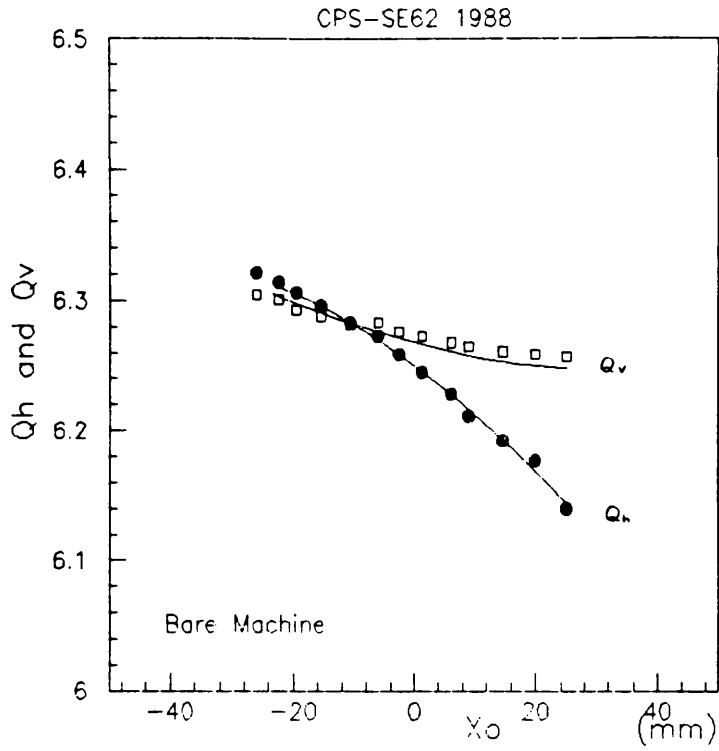


Fig. 2a: Q vs X_o

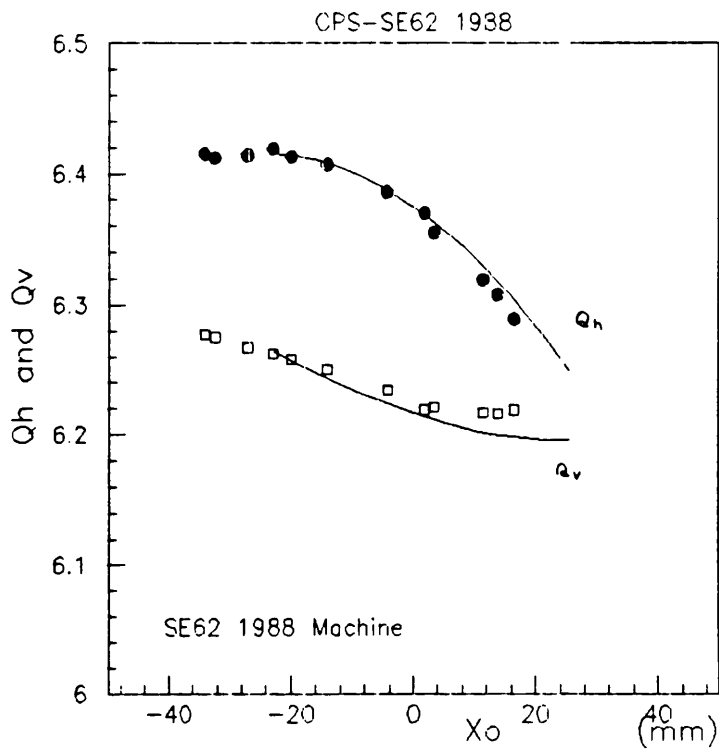


Fig. 2b: Q vs X_o

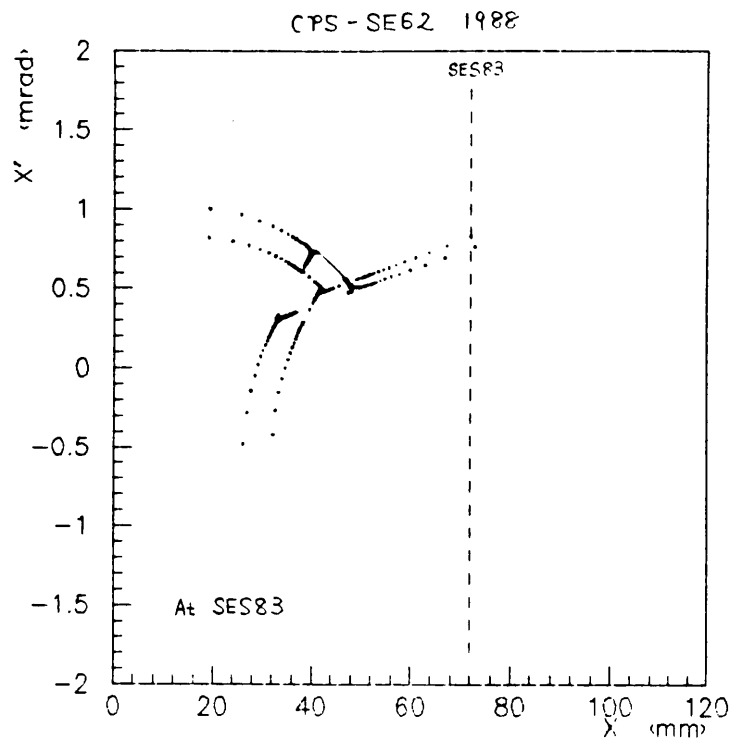


Fig. 3a: PS resonant extraction

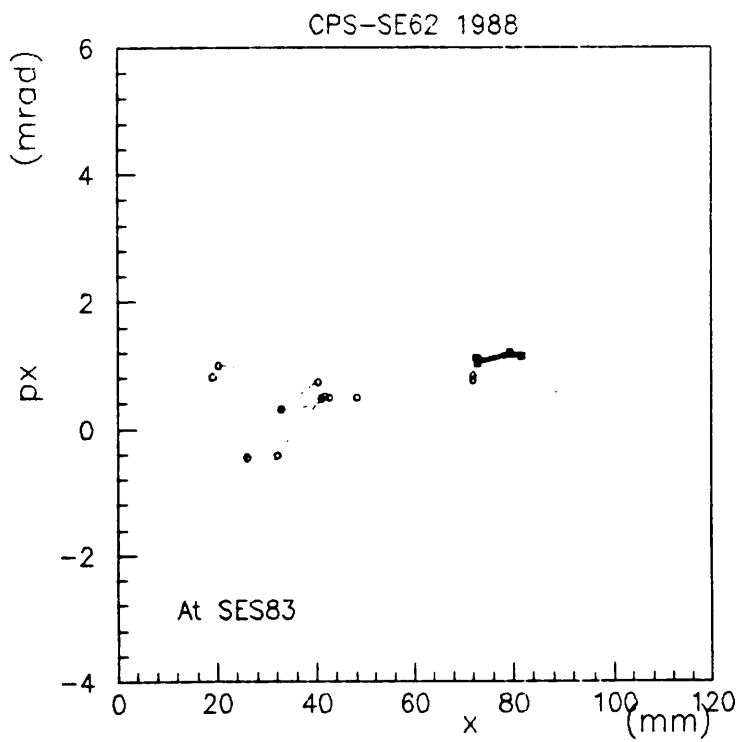


Fig. 3b: SE62-1988 (at SES83)

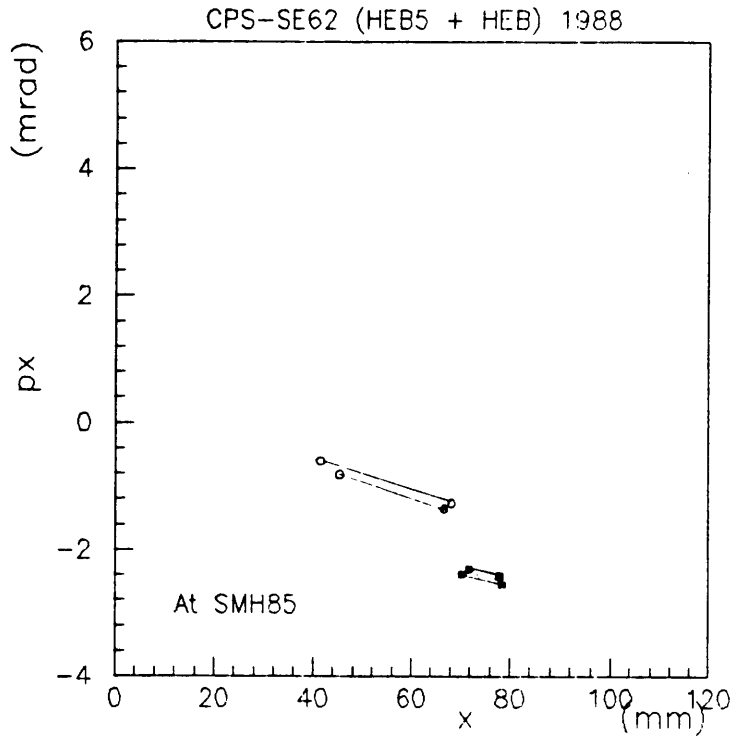


Fig. 3c: SE62-1988 (at SMH85)

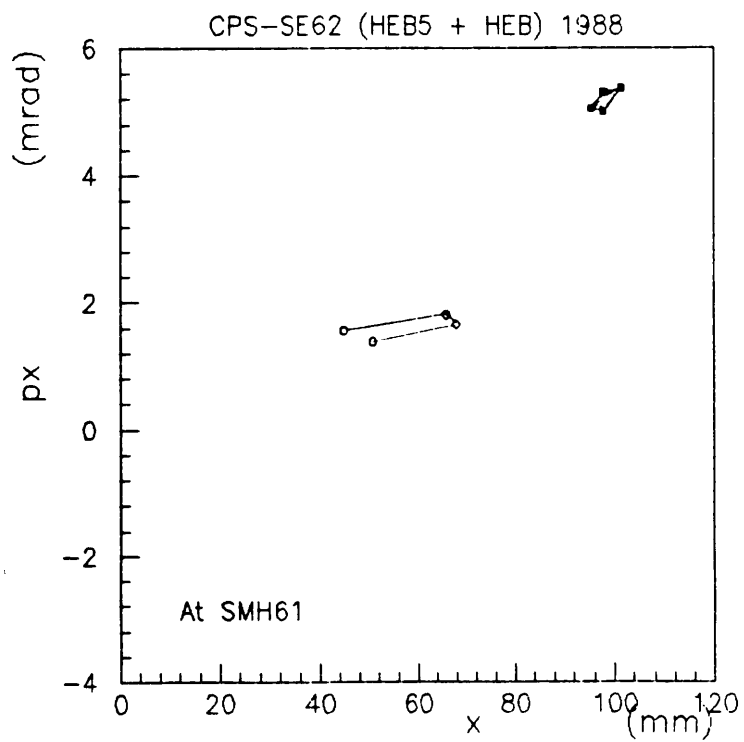


Fig. 3d: SE62-1988 (at SMH61)

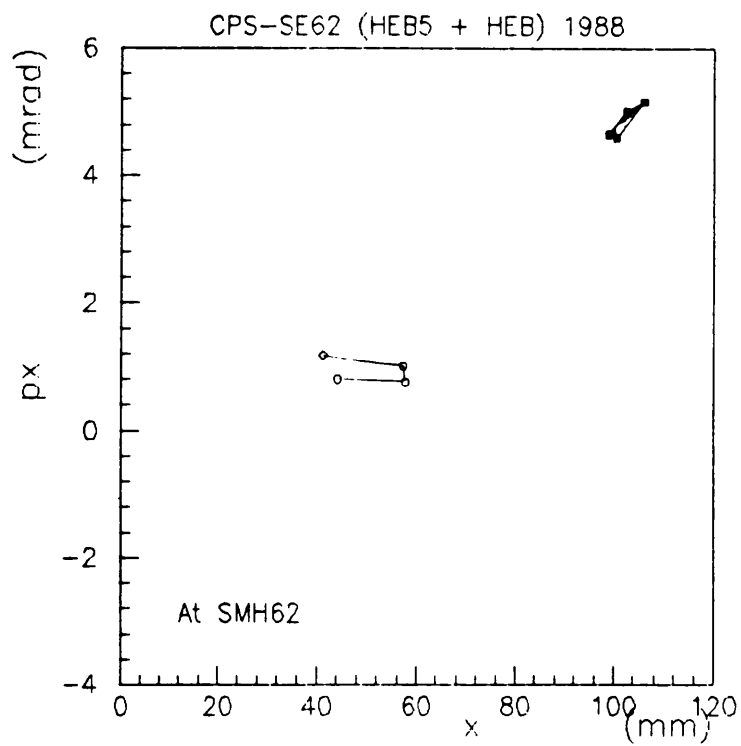


Fig. 3e: SE62-1988 (at SMH62)



Photo No. 1: QFO 01 = 610 A



Photo No. 2: QFO 01 = 400 A



Photo No. 3: QFO 01 = 300 A

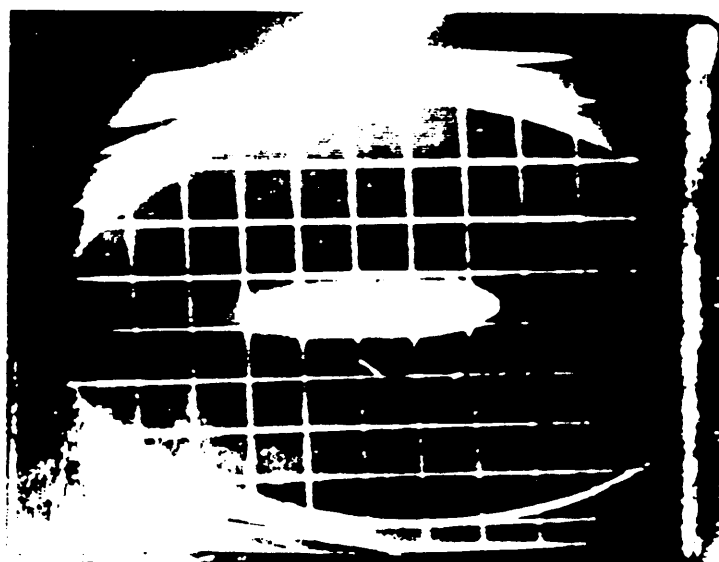


Photo No. 4: QFO 01 = 0 A

Fig. 4:
Beam spot size at FT62 MTV02 as a
function of the current in QFO 01

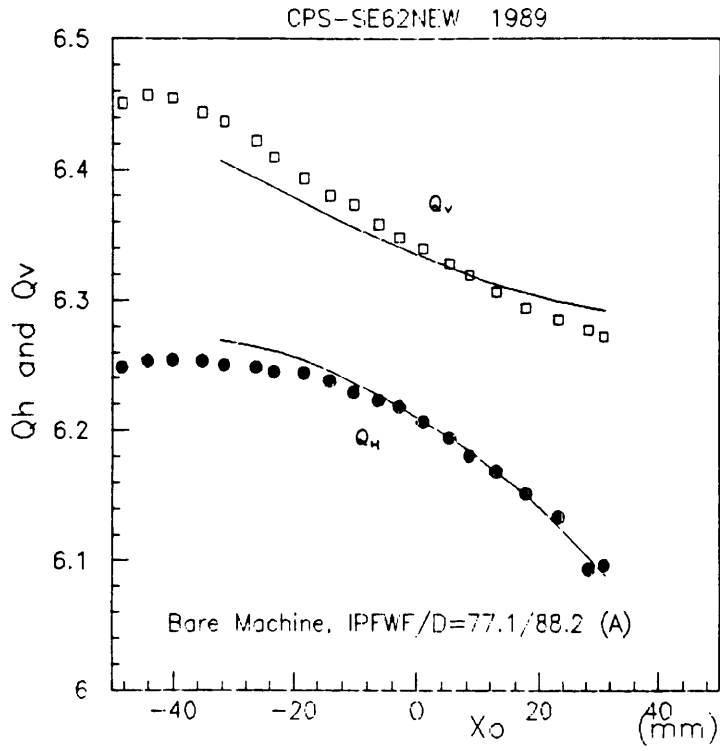


Fig. 5a: Q vs X_o

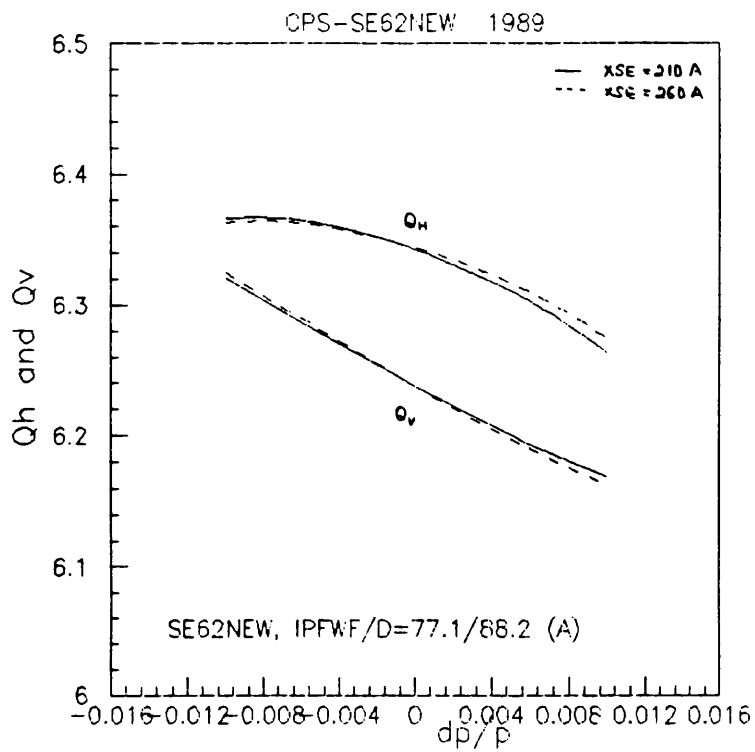


Fig: 5b: Q vs dp/p

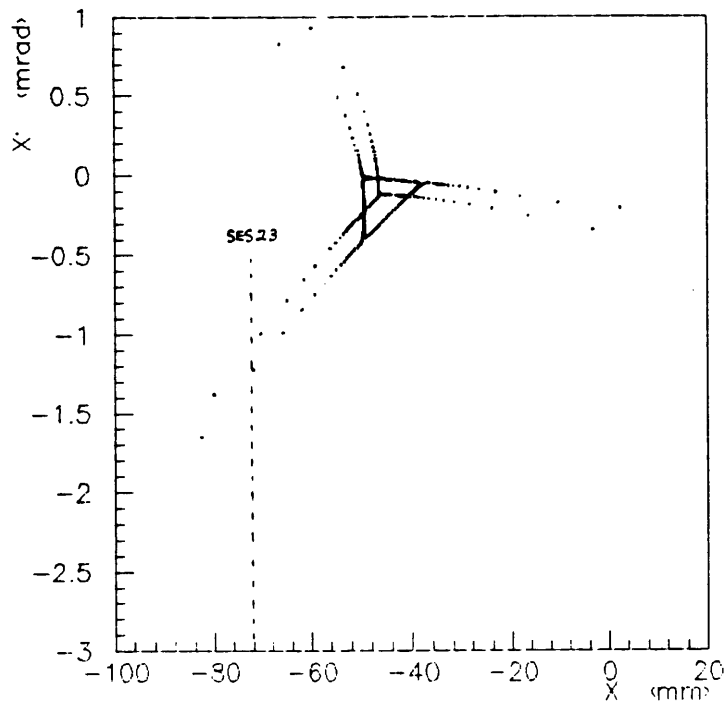


Fig. 6a: PS resonant extraction

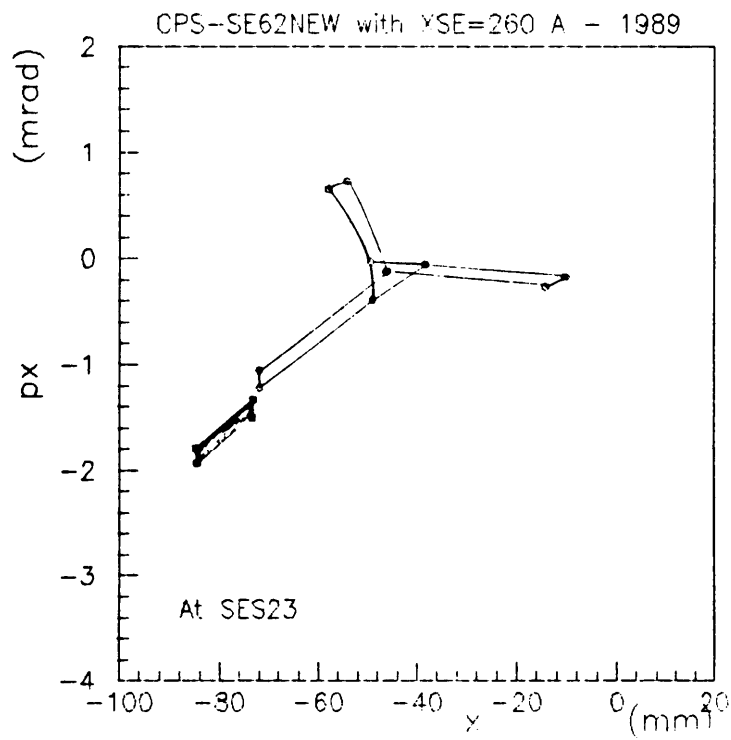


Fig. 6b: SE62NEW (at SES23)

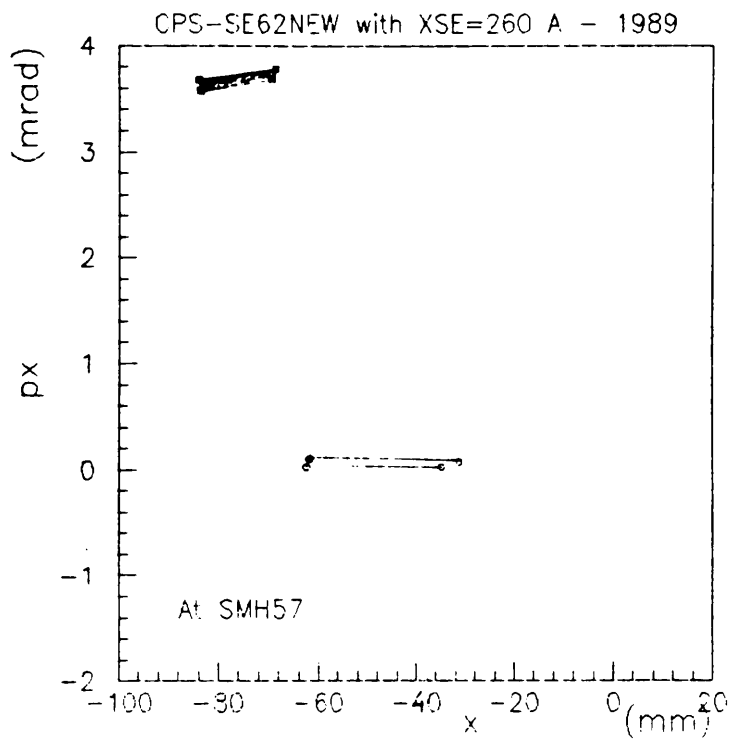


Fig. 6c: SE62NEW (at SMH57)

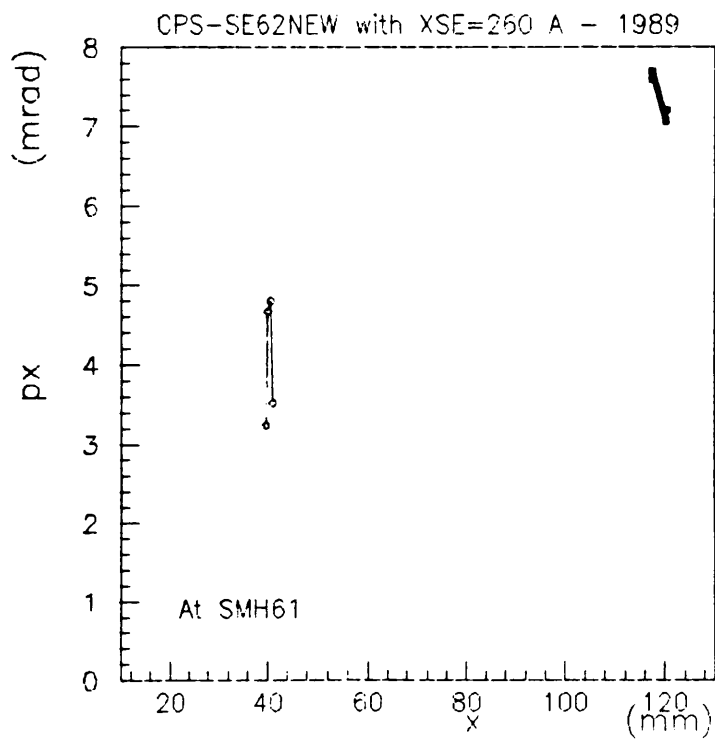


Fig. 6d: SE62NEW (at SMH61)

Distribution (open)

Distribution (of abstract
PS, SPS and LEP Scientific Staff
/ed